Finite Difference Analysis of an Open-Ended, Coaxial Sensor Made of Semi-Rigid Coaxial Cable for Determination of Moisture in *Tenera* Oil Palm Fruit

E. M. Cheng [1], Z. Abbas [2], MohamedFareq AbdulMalek [3], K. Y. Lee [4], K. Y. You [5], S. F. Khor [6], J. Hassan [2], and H. Zainuddin [2]

[1] School of Mechatronic Engineering,
Universiti Malaysia Perlis (UniMAP), Pauh Putra Campus, 02600 Arau, Perlis, Malaysia
emcheng@unimap.edu.my

[2] Physics Department, Faculty of Science
Universiti Putra Malaysia, 43400 Serdang, Selangor, Malaysia
za@upm.edu.my, jumiah@upm.edu.my, hishamuddin@upm.edu.my

[3] Faculty of Engineering and Information Sciences
University of Wollongong in Dubai, Al Sufouh Streetو Dubai Knowledge Village - إمارة دبيّ - United Arab Emirates
mohamedfareqmalek@uowdubai.ac.ae

[4] Department of Electrical and Electronic Engineering, Faculty of Engineering and Science
Tunku Abdul Rahman University, 53300 Setapak, Kuala Lumpur, Malaysia
kylee@utar.edu.my

[5] Radio Communication Engineering Department (RaCED), Faculty of Electrical Engineering
Universiti Teknologi Malaysia, Skudai, Johor 81310, Malaysia
kyyou@fke.utm.my

[6] School of Electrical Systems Engineering
Universiti Malaysia Perlis (UniMAP), Pauh Putra Campus, Arau, Perlis 02600, Malaysia
sfkhor@unimap.edu.my

Abstract ─ In this paper, the use of the Finite Difference Method (FDM) is proposed to determine the reflection coefficient of an open-ended coaxial sensor for determining the moisture content of oil palm fruit. Semi-rigid open-ended coaxial sensor is used in conjunction with Vector Network Analyzer for reflection coefficient measurement of oil palm fruit. Moisture content in oil palm fruit determine optimum harvest time of oil palm fruit. Finite difference method is then used to simulate measured reflection coefficient due to different moisture contents in oil palm fruit at various stages of ripeness. The FDM results were found to be in good agreement with measured data when compared with the quasi-static and capacitance model. Overall, the mean errors in magnitude and phase for the FDM were 0.03 and 3.70°, respectively.

Index Terms ─ Finite difference method, moisture content, oil palm fruit, open-ended coaxial sensor, reflection coefficient.

I. INTRODUCTION

A. Background of oil palm

The oil palm, *Elaeis guineensis Jacq*, is indigenous to West Africa where the cultivation area is from Sierra Leone, Liberia, the Ivory Coast, Ghana, Cameroon and extended to the equatorial regions of the Republics of Congo and Zaire [1].

The harvesting period begins around 24 to 30 months after planting [2] and each palm can produce between 8 to 15 fresh fruit bunches (FFB) per year. The weight of each bunch is about 15 to 25 kg each and this depends on the planting material and age of the palm. Each FFB contains about 1000 to 1300 fruit. Each fruit consists of 3 layers, which are the fibrous mesocarp layer, the endocarp (shell) and the kernel (Fig. 1).

Palm oil is obtained from the fleshy mesocarp, which is composed of 45-55 per cent oil by weight [3]. The *Tenera* has been the preference for the palm oil industry because of its thin shell and high oil content in the thick mesocarp structure.

Submitted On: July 22, 2015
Accepted On: July 4, 2016

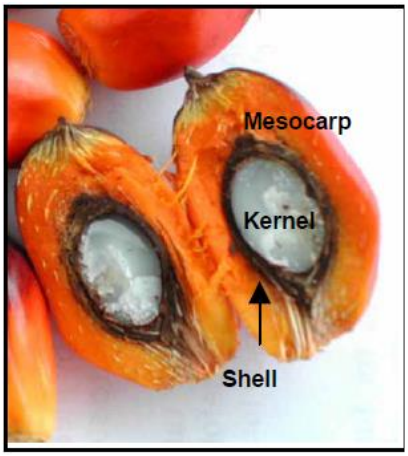

Fig. 1. Cross section of a fruitlet [2].

B. Conventional technique of determining the fruit ripeness

There are several techniques to gauge the oil palm fruit ripeness. The visible symptoms to determine fruit ripeness include the color change of the fruit [4]-[5], the percentage or number of detached fruit per bunch [6] and the fruit ability to float on water, or so called floatation technique [7]. However, they are unreliable due to their inconsistencies and inaccuracies.

C. The relationship between moisture content and ripeness of oil palm fruit

The current research in gauging the ripeness of oil palm fruit is via examination of the amount of moisture content in mesocarp of an oil palm fruit. Ariffin et al. [8] states that the moisture content in mesocarp of oil palm fruit can be used as an indicator to determine the fruit ripeness. It was found that the moisture content is higher in unripe oil palm fruit at the early stage of fruit development. The water in the mesocarp decreases gradually during fruit ripening which coincides with the oil accumulation approximately from week 12 to week 15 after anthesis (Fig. 2). The amount of water in fresh mesocarp decreases rapidly to 40% in the ripe fruit from week 16 to week 17 after anthesis. The water content will then decreases slowly from week 18 to week 24. The moisture content decrease is almost about the same time as the accumulation of oil in the mesocarp. Hence, there is a close relationship between the moisture content (mc) and oil content (oc) in mesocarp. This phenomenon is helpful to gauge the fruit ripeness. Hartley [1] states that the mass fraction of oil and mass fraction of water in the mesocarp can be expressed linearly. This relationship are visualize in Fig. 3.

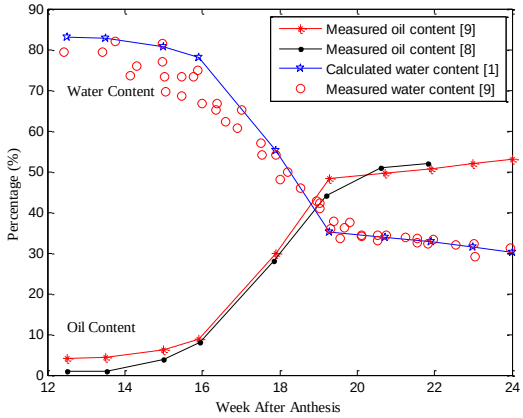

Fig. 2. Variation in moisture content and oil content after anthesis.

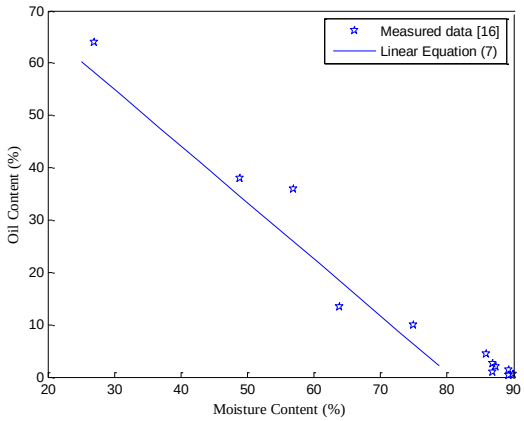

Fig. 3. The correlation of the water content (moisture content) against the oil content in mesocarp.

II. MATERIALS AND METHOD

A. Measurement of moisture content in oil palm fruit

For the sake of establishing the relationship between reflection coefficient and moisture content, the actual moisture content must first be determined by a reliable technique. Standard oven method was chosen to determine moisture content in palm oil fruit because it is the method proposed by Malaysia Palm Oil Board (MPOB). The relative moisture content of oil palm fruit, in percentage (wet basis) can be expressed as equation (1):

$$\text{m.c.} = \frac{m_{\text{before dry}} - m_{\text{after dry}}}{m_{\text{before dry}}} \times 100\% , \qquad (1)$$

where $m_{\text{before dry}}$ and $m_{\text{after dry}}$ are the weight of fruit sample before dried and after dried, respectively.

B. Simulation and measurement of open-ended coaxial sensor on oil palm fruit

Open-ended coaxial sensors have been used extensively to measure the reflection coefficient of oil palm fruit [10]-[12]. The probe associated with such a sensor is made of an RG-402 semi-rigid cable, normally operating at 2 GHz. The stage of fruit ripeness is determined by the percentage of moisture content. As the moisture content (or permittivity, ε_r^*) of the fruit changes, the values of reflection coefficient measured by the sensor also changed.

Unfortunately, both the quasi-static model (a.k.a. the admittance model) and the capacitance model assume that the thickness of the sample under consideration is infinite [13]. Therefore, these models are inappropriate for characterizing a thin sample or any sample with finite thickness, such as oil palm fruit. However, the dimensions of the sample must be taken into account in FDM calculation [14]-[15]. For instance, the length and thickness of the fruit are considered in FDM.

C. The moisture content and the dielectric properties in oil palm fruit

The moisture content of agricultural products is one of the most important parameters for determining the quality of the products. This information is required to determine the optimum time for harvesting and safe storage.

The standard oven-drying method is tedious and time-consuming, and they are not suitable for use in agro-production application. Hence, the development of a rapid test method, such as microwave method, is a pressing need in the industry. The complex dielectric permittivity, ε^* is often expressed by equation (2):

$$\varepsilon^* = \varepsilon' - j\varepsilon'', \tag{2}$$

where ε' is related to the ability of the material to store energy (dielectric constant) and ε'' is the loss factor which is the dissipation of energy in the material. The permittivity of oil palm fruit [17] can be expressed as:

$$\sqrt{\varepsilon^*} = v_w\sqrt{\varepsilon_w^*} + v_f\sqrt{\varepsilon_f^*} + v_0\sqrt{\varepsilon_0^*}, \tag{3}$$

where v_w, v_f, and v_0 are the volume fraction of water, fiber, and oil, respectively, and ε_w^*, ε_f^*, and ε_0^* are the corresponding complex permittivities. It has been shown that both ε_f^* and ε_0^* are essentially constant throughout the frequency range between DC and 10 GHz with ε_f^* = 2.2 - 0.06j and ε_0^* = 2.3 - 0.02j. The values of ε_w^* are obtained from the Cole-Cole model [18]:

$$\varepsilon_w^* = \varepsilon_\infty + \frac{\varepsilon_s - \varepsilon_\infty}{1 + (j\omega\tau)^{1-\alpha'}}, \tag{4}$$

where α' is the distribution parameter, which is an empirical constant. Thus, the palm oil mixture consists of three main components, i.e., v_o, v_w, and v_f, and the relationship between them is:

$$v_0 = 1 - v_w - v_f. \tag{5}$$

Since v_f = 0.16 [1], v_w can be calculated as:

$$v_w = \frac{(\text{m.c.})(\rho_f v_f + \rho_0 - \rho_0 v_f)}{\rho_w - (\text{m.c.})\rho_w + (\text{m.c.})\rho_0}, \tag{6}$$

where the densities ρ_w, ρ_f and ρ_0 are 1, 0.92 and 0.93 respectively and mc is the moisture content. The volume fraction of oil and water can be found by using Equation (5) and Equation (6), respectively. In Equation (7), the relative moisture content in the wet basis can be determined in terms of the mass of water, oil, and fiber, which are represented by m_w, m_0, and m_f, respectively [19]:

$$\text{m.c.} = \frac{m_w}{m_w + m_0 + m_f} \times 100\%. \tag{7}$$

Hence, the permittivity of the oil palm fruit can be calculated using the mixture model [12].

Figure 4 shows the permittivity of oil palm fruit for *mc* between 20% and 90%. The abnormal behavior of ε' with *mc* below 30% is due to bound water [20]-[21].

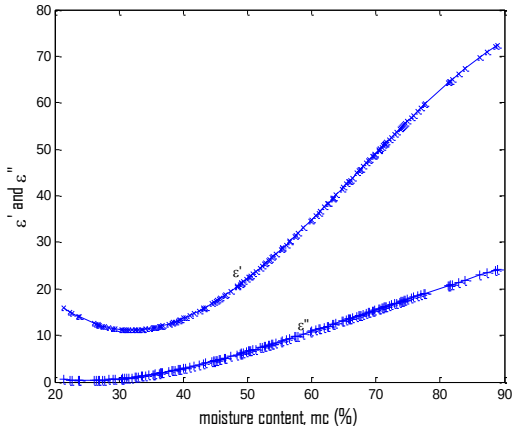

Fig. 4. Relationship of moisture content in oil palm fruit with ε' (dielectric constant) and ε'' (loss factor) at 2 GHz.

D. Admittance model (quasi-static model)

The relationship between normalized admittance and the reflection coefficient of an open-ended, coaxial sensor can be written as Equation (8):

$$\Gamma = \frac{Z_L - Z_0}{Z_L + Z_0} = \frac{1 - \tilde{Y}_L}{1 + \tilde{Y}_L}, \tag{8}$$

where Z_0 is the 50 Ω characteristic impedance of the coaxial sensor. The normalized admittance, $\tilde{Y}$ [12], [22], is established by two terms, i.e., normalized conductance, $G(0)/Y_0$, and susceptance $B(0)/Y_0$. $\tilde{Y}$ can be expressed as:

$$\tilde{Y} = \frac{G(0)}{Y_0} + j\frac{B(0)}{Y_0}, \quad (9)$$

where

$$\frac{G(0)}{Y_0} = \frac{\sqrt{\varepsilon_r}}{\ln\left(b/a\right)\sqrt{\varepsilon_c}} \int_0^{2\pi} \frac{1}{\sin\theta} \times \left[J_o\left(k_o\sqrt{\varepsilon}b\sin\theta\right) - J_o\left(k_o\sqrt{\varepsilon}a\sin\theta\right)\right]^2 d\theta, \quad (10)$$

$$\frac{B(0)}{Y_0} = \frac{\sqrt{\varepsilon}}{\pi\ln\left(b/a\right)\sqrt{\varepsilon_c}} \times \int_0^{\pi} \begin{bmatrix} 2Si\left(k_o\sqrt{\varepsilon\left(a^2+b^2-2ab\cos\theta\right)}\right) \\ -Si\left(2k_o\sqrt{\varepsilon}a\sin\left(\frac{\theta}{2}\right)\right) \\ -Si\left(2k_o\sqrt{\varepsilon}b\sin\left(\frac{\theta}{2}\right)\right) \end{bmatrix} d\theta, \quad (11)$$

where ε_c is the dielectric constant of the material that fills the coaxial line, ε is the dielectric constant in the external medium, *a* and *b* are the inner and outer radii, respectively, k_o is the free space propagation constant, J_o is the zero-order Bessel function, and *Si* is the sine integral. Equations (10) and (11) can be approximated by the first term of the Taylor series expansion [22]. In this study, the aspect ratio, b/a was 3.2981.

E. Capacitance model

An open-ended coaxial sensor can be used to measure the dielectric constant of living tissue (*in vivo*), e.g., oil palm fruit. The expression that represents the aperture admittance in terms of the *in vivo* measurement of the relative permittivity of the external medium [13] is:

$$Y_L(\omega, \varepsilon_r^*) = j\omega(\varepsilon_r^* C_0) = j\omega C(\varepsilon_r^*), \quad (12)$$

in which

$$C(\varepsilon_r^*) = \varepsilon_r^* C_0, \quad (13)$$

$$C(\varepsilon_r^* = 1) = C_0, \quad (14)$$

$$C_0 = 2.38\varepsilon_0(b-a), \quad (15)$$

$$\varepsilon_0 = \frac{10^{-9}}{36\pi}\ \text{F/m}, \quad (16)$$

where Y_L is the admittance at the end of the coaxial probe, ω is the angular frequency, ε_0 is the permittivity of free space, ε_r^* is the relative permittivity of the sample that occupies the space outside the coaxial line, and C_0 is the capacitance of the probe (in free space). The fringing capacitance, $C(\varepsilon_r^*)$ at the aperture of the probe consists of a part that is dependent on the relative permittivity of the sample and the filling of the coaxial line.

F. Iteration method in solving finite difference method (FDM)

The computation work of FDM involves large system of simultaneous equations, and iterative method was used to overcome these. Iterative method uses the approximation from previous computation to calculate the next approximation. This computation is carried out iteratively until its value converges.

Initial values of the potentials were set at the free nodes which equals to zero or to any reasonable value. For example, we set 1 V at the excitation plane and 0 V at the ground conductor or perfect electric conductor (PEC). These potential values are arranged to form a matrix. Maintaining the potentials at the fixed nodes constant at all times, then applying the equation:

$$V_{i,j} = \frac{1}{4}\left(V_{i+1,j} + V_{i-1,j} + V_{i,j+1} + V_{i,j-1}\right), \quad (17)$$

to every free node in turn until the potentials at all grid nodes (Fig. 5) are calculated. The potential in output matrix is fed to the input matrix to calculate the potential (element in matrix) in the next iteration. The potentials obtained at first iteration may only provide an approximate result because the first iteration may not able to converge the potential to a correct value. In order to enhance the accuracy of the potentials, the calculation was repeated at each free node using previously calculated potential. The iterative modification of the potential at each grid node or vertex points of meshes is repeated until desired degree of accuracies is obtained or until two successive values at each node are sufficiently equal.

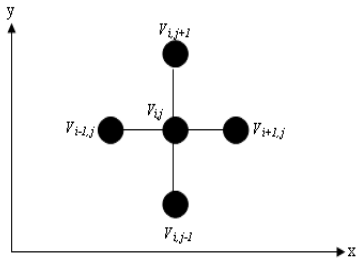

Fig. 5. Finite difference solution pattern: finite-difference, five-node molecule.

G. Application of the concept of finite-difference in the coaxial sensor and sample

Plane CD is the boundary between two different materials, i.e., the Teflon in the coaxial line and the sample. At the dielectric boundary (Fig. 6), the boundary condition,

$$D_{1n} = D_{2n}, \quad (18)$$

must be imposed where D_{1n} and D_{2n} are the normal components of the electric flux density at dielectric filler in coaxial line and in the sample being tested, respectively. This condition is based on Gauss' Law for electric fields, i.e.,

$$\oint D \cdot dl = \oint \varepsilon E \cdot dl = Q_{enc} = 0, \quad (19)$$

since no free charge is deliberately placed on the dielectric boundary. Substituting $E = -\nabla V$ in Equation (19) gives:

$$0 = \oint \varepsilon \nabla V \cdot dl = \oint \varepsilon \frac{\partial V}{\partial n} \cdot dl, \quad (20)$$

where $\frac{\partial V}{\partial n}$ denotes the derivative of V normal to the contour *l*. Applying Equation (20) to the interface in Fig. 6 yields:

$$V_0 = \frac{\varepsilon_1}{2(\varepsilon_1+\varepsilon_2)} V_1 + \frac{\varepsilon_2}{2(\varepsilon_1+\varepsilon_2)} V_3 + \frac{1}{4} V_2 + \frac{1}{4} V_4. \quad (21)$$

The finite difference potential results on plane CD in Fig. 6 (circular ring potential in the area of the cross section of coaxial sensor, V_{ring}) were computed. The total potential, V_{area}, and the total charge, Q_{area}, at the area of the aperture of the probe can be determined easily by using Equations (22) and (23), respectively [23]:

$$V_{area} = \int_a^b V_{ring}\, d\rho, \quad (22)$$

$$Q_{area} = \varepsilon \int_a^b \int_0^{2\pi} \frac{V_{ring}}{\rho} \rho d\phi\, d\rho, \quad (23)$$

where ρ is the radius at aperture of the coaxial probe, *a* is the inner radius of the coaxial probe, and *b* is the outer radius of the coaxial probe. The normalized and characteristic admittance are expressed as:

$$\tilde{Y} = \frac{j\omega C}{Y_0}, \quad (24)$$

$$\tilde{Y}_0 = \frac{2\pi}{\sqrt{\frac{\mu_0}{\varepsilon_0 \varepsilon_c}} \cdot ln\left(\frac{b}{a}\right)}, \quad (25)$$

where ε_0 is the permittivity in free space, ε_c is the relative permittivity of the coaxial line (PTFE), and μ_0 is the free space of permeability. The reflection coefficient, Γ is obtained from Equation (8).

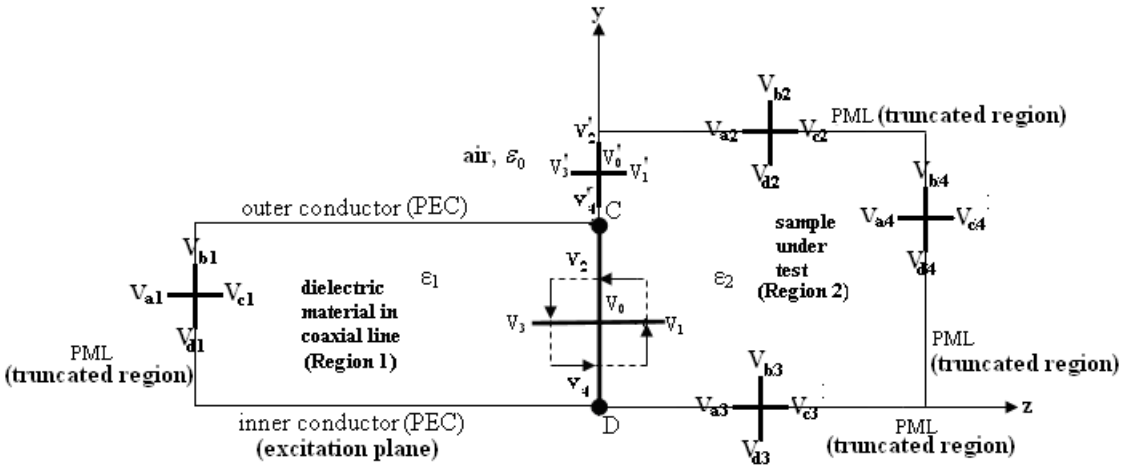

*PML=Perfect Matched Layer
PEC=Perfect Electric Conductor

Fig. 6. Interface between media of dielectric permittivities ε_1 (dielectric material in the coaxial line) and ε_2 (sample being tested).

III. RESULTS AND DISCUSSION

A. Magnitude of the reflection coefficient

The results comparison for the measured and calculated values of the reflection coefficient at various percentages of moisture content in oil palm fruit is shown in Fig. 7.

The whole results suggested that the magnitude of the reflection coefficient decreases as the moisture content of the fruit increased [24]. The results obtained using the mixture model indicated that complex permittivity, ε* increased when the moisture content is high. This relationship, which is due to the high degree mismatch of impedance, is clearly shown in Fig. 8. Increases in ε* could cause the sample's impedance, Z_L to decrease. The admittance model can be used to calculate this.

In summary, increasing the moisture content causes the complex permittivity to increase, as Fig. 4 shows. Hence, this condition results in the decrease of impedance, which, in turn, causes the magnitude of the reflection coefficient, $|\Gamma|$, to decrease. Figure 8 shows this relationship as a 3D line plot.

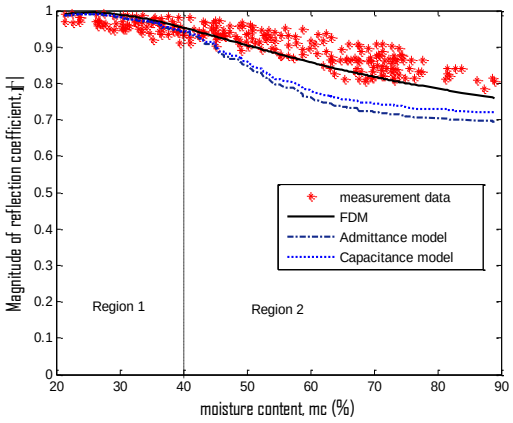

Fig. 7. The comparison between measured $|\Gamma|$ with calculated results obtained from finite difference method (FDM), admittance model and capacitance model at 2 GHz.

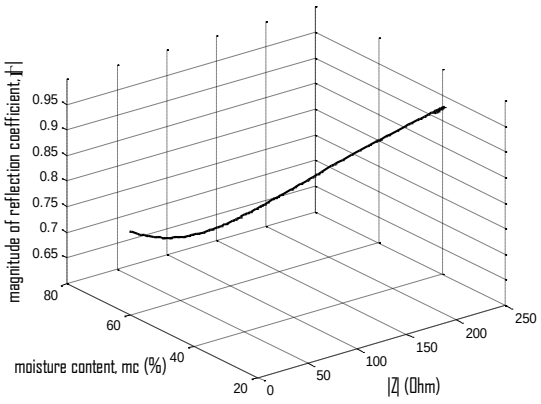

Fig. 8. The relationships between $|Z_L|$, $|\Gamma|$, and moisture content.

According to the admittance model, decreasing Z_L (as a result of a greater dielectric constant) results in a decrease in the magnitude of the reflection coefficient. The relationship between the normalized admittance, $\left(\tilde{Y}_L = \frac{Z_0}{Z_L}\right)$ and the reflection coefficient, Γ is shown by the Equation (25). Z_0 is the 50 Ω characteristic impedance of the coaxial sensor. Figure 8 shows the relationship between magnitude of reflection coefficient, magnitude of impedance, and moisture content.

The FDM, admittance model and capacitance model produced trends that were similar to the measurement results. The magnitudes that were acquired by FDM showed better agreement with the measured data than the admittance model or the capacitance model [19]. The FDM provided a mean error of 0.03 for the moisture content ranging from 20% to 90%. The mean errors produced by the admittance model and the capacitance model are 0.06 and 0.05, respectively. The poor accuracies of the admittance model and the capacitance model were due to the assumptions that were made in the models. In both models, it is assumed that the thickness of the sample is infinite [13]. Therefore, neither one of them is suitable for use in characterizing a thin sample or any sample with a finite thickness, such as the sample of oil palm fruit. However, the dimensions of the sample, i.e., its length and width, must be taken into account in the FDM calculation. The PML is necessary to truncate the computation region of the material, in order to retain the practicability of the computation.

Among the three models, the FDM approach had the best agreement with the measured values of the reflection coefficient, as shown in Fig. 7.

Figure 9 represents a portion of Fig. 7, which designated as region 1 in Fig. 7. Region 1 is in mc range from 20% to 40%. Meanwhile, the region where the mc range is from 40% to 90% is designated as region 2. These two mc ranges are important to study the period after anthesis. The relationship of water content in fruit and the period after anthesis can be referred to Fig. 2.

Measurement data shows $|\Gamma|$ decreases gradually when moisture content increases. Referring to Fig. 2, it can be observed that the mc in the range of 20% to 40% is within 18 weeks to 24 weeks after anthesis. During this period, the water content and oil content show insignificant change. The fruit accumulates maximum amount of oil content in this mc range. It can be used to determine the optimum of harvesting time of oil palm fruit. Therefore, the relationship of $|\Gamma|$ against moisture content can be used to predict moisture content upon the knowledge of $|\Gamma|$.

The trend line in Fig. 2 that represents water and oil content seems unchanged in this mc range. The fruit seems to be at constant water and oil level. The mean magnitude error of FDM, admittance model and capacitance model are similar, i.e., 0.01 when compared with Fig. 9. The similar values of mean magnitude error for these models are close to the mean magnitude error that is presented by the fitting line shown in Fig. 9, i.e., 0.01. The insignificant change in moisture content yield to the insignificant change in their magnitude of reflection coefficient as well. It can be proved by the sensitivity in Fig. 10. Figure 10 indicates the sensitivity of $\frac{d|\Gamma|}{d(mc)}$ in region 1. It can be noticed that the sensitivity is kept constant when the mc increases from 20% to 40%. It means that it is best represented as a linear relationship. It has been proved by the fitting linear equation in Fig. 9. The sensitivity value is -0.0017 and it is very small. This can be explained by Fig. 2. In Fig. 2, the range of water content which is between 20% to 40% shows the insignificant change when the fruit exceeds week 17 after anthesis.

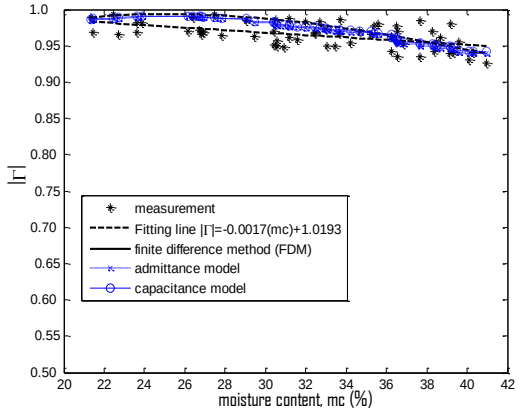

Fig. 9. Region 1 of Fig. 7.

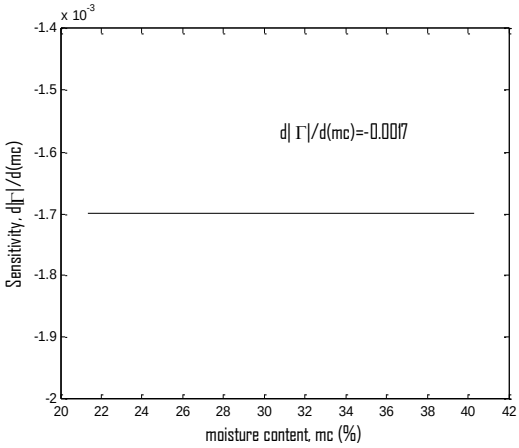

Fig 10. Sensitivity of $\frac{d|\Gamma|}{d(mc)}$ for the mc range between 20% to 40% (region 1).

Figure 11 represents region 2 in Fig. 7. The range 40% to 90% moisture content is within week 12 to week 16 after anthesis. It can be observed in Fig. 2 as well. The water content and oil content change drastically during week 16 to week 17. The water content starts to decrease, whereas oil content starts to rise on week 16 after anthesis. This is difficult to predict because the moisture content has an abrupt change. Hence, it can be observed that the error of FDM, admittance model and capacitance model are larger than the case in region 1 (Fig. 9), namely 0.06, 0.11 and 0.10. When FDM, admittance model and capacitance model are compared to each other, it can be found that FDM shows the best agreement with measured data with the smallest error, 0.06 during week 12 to 17 after anthesis. The fitted line of measure data is best represented as quadratic equation $|\Gamma| = (6\times10^{-6})(mc)^2 - 0.004(mc) + 1.111$. Hence, the sensitivity equation [25] can be represented by $\frac{d|\Gamma|}{d(mc)} = (1.2\times10^{-7})(mc) - 0.004$ and it is visualized in Fig. 12. Even though the sensitivity decreases when the moisture contents increases from 40% to 90%, however, the variation of sensitivity with mc is not drastic. Although the sensitivity decreases, it is still greater than the sensitivity in region 1 as shown in Fig. 10. Overall, the sensor has higher sensitivity $\frac{d|\Gamma|}{d(mc)}$ for moisture content greater than 40% (region 2) if compared with Fig. 10 and it is commendable as this coincides with the drastic change in moisture content from unripe fruits to the ripe stage.

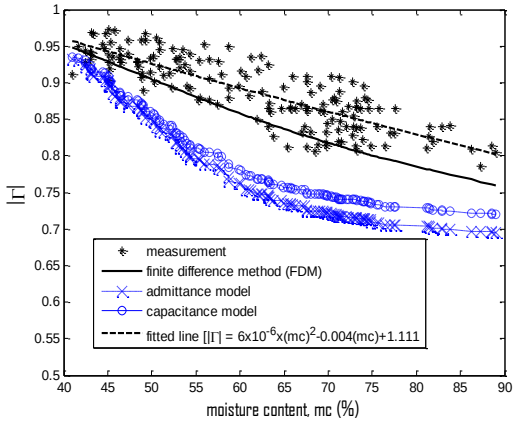

Fig. 11. Region 2 of Fig. 7.

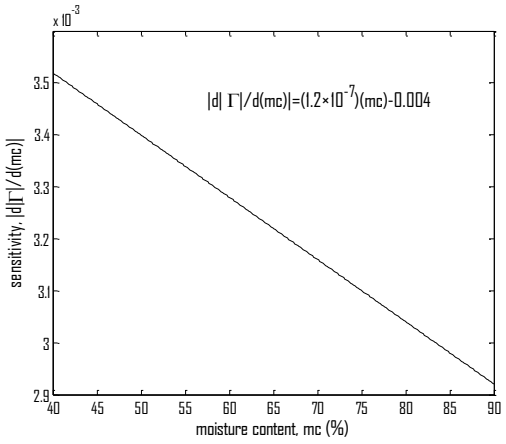

Fig. 12. Sensitivity of $\frac{d|\Gamma|}{d(mc)}$ for the mc range between 40% to 90% (region 2).

B. Phase of reflection coefficient

The variation of phase with moisture content, *mc*, is shown in Fig. 13. Phase is highly influenced by the complex permittivity, ε* and the thickness of the sample

[26]. In addition, the length of the coaxial line and the thickness of the fruit can cause a phase shift. The phase shift in Fig. 13 shows good agreement with the measured data when compared with the phase on plane AB. When the length of coaxial line varies from 0.5 cm to 10 cm, it can be observed that the error in FDM shows the smallest when the length is 6 cm as seen in Fig. 14. However, the measured length of coaxial sensor from the caliper shows 5.655 cm. This deviation may be due to the inhomogenity of the fruit in terms of permittivity. The FDM results deviated from the measured data because FDM only considers a homogeneous sample calculation. The phase of reflection coefficient from FDM still shows the best results for 6 cm coaxial sensor when compared to admittance model and capacitance model which have extended to plane AB as well by using technique of de-embedding of coaxial probe [27]. The effects of length of the open-ended, coaxial sensor towards reflection coefficient in reflection measurement had been reported [28]. Error shown by FDM is 45.6 degrees on the plane CD. After the plane is extended from plane CD to AB, the error is reduced to 7.80 degrees with similar condition. It is expected that the measurement plane must coincide with the calibration plane, since the calibration is done on plane AB. The mean phase error of admittance model (25.0 degrees of mean error) and capacitance model (27.1 degrees of mean error) are higher at plane CD if compared with the mean phase error at plane AB. After the plane CD is extended to plane AB, the error of admittance model is reduced to 17.3 degrees, while capacitance model is reduced to 15.0 degrees. After the comparison was done, the FDM on plane AB shows the best agreement with measured data. The poor accuracy in admittance model and capacitance model are due to the assumption made in both models. As mentioned previously, the admittance model and capacitance model assumed that the thickness of sample under consideration is infinite [13]. Therefore, they are not suitable to be used in characterizing a thin sample or any sample with finite thickness which is similar with oil palm fruit. This deviation of measured phase from the calculated phase using FDM may be due to the inhomogeneity of the oil palm fruit. The FDM results deviated from measured data because the FDM calculations only considered homogeneous samples. The FDM approach has better results for the phase of the reflection coefficient than the admittance model or the capacitance model. FDM has an error of only 3.70 degrees for similar conditions. The mean phase errors of the admittance model and the capacitance model were approximately 18 degrees and 15 degrees, respectively. When all the results were compared, it was apparent that the FDM provided the best agreement with the measured data. The poor accuracies in the admittance model and the capacitance model were due to the limiting assumptions that were made in both models. As mentioned previously, in both of these models, it was assumed that the thickness of sample of fruit was infinite. Therefore, neither of these two models is suitable for characterizing thin sample or any sample with finite thickness, such as the oil palm fruit. Figure 15 represents region 1 in Fig. 13. In Fig. 9, the magnitude of measured data, admittance model and capacitance model shows insignificant change with moisture content range 20% to 40%. The phase of admittance model and capacitance model for moisture content between 20% and 40% is almost constant as shown in Fig. 15. However, the measured phase decreases with equation $\phi = 0.0117(\text{mc})^2 - 1.2846(\text{mc}) - 30.665$. The mean phase error for FDM, admittance model and capacitance model on plane AB are 3.59 degrees, 4.27 degrees and 4.44s degree respectively. They have the mean phase error that is close to the fitting line which shows 3.13 degrees of mean error. Comparing FDM with admittance model and capacitance model, FDM has better agreement with the measured phase. The FDM, admittance model and capacitance model on plane CD (measurement plane) show a larger mean phase error if compared with the models on plane AB. It is due to the measured magnitude are collected on calibration plane but not the measurement plane. The differentiation of the fitting line equation with moisture content is:

$$\left|\frac{d\phi}{d(\text{mc})}\right| = 0.0234(\text{mc}) - 1.2846, \qquad (26)$$

or so-called sensitivity for moisture content range 20% to 40% as shown in Fig. 16. It is dissimilar to Fig. 10 because of the sensitivity in Fig. 16 decreases from 0.3 to 0.8 for moisture content range 20% to 40%, however, the sensitivity in Fig. 16 decreases insignificantly from 0.0035 to 0.0029. For this reason, the measured phase has higher sensitivity than the measured magnitude in region 1.

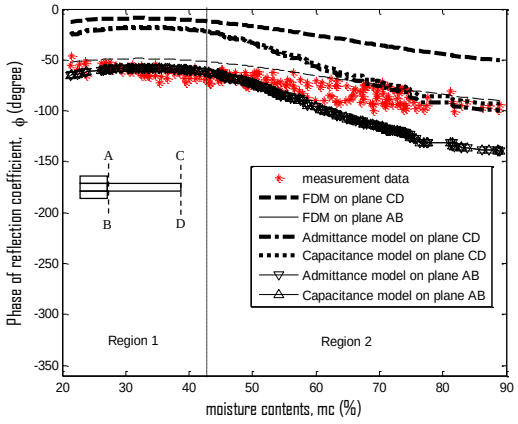

Fig. 13. Comparison of phase of reflection coefficient among measured data, FDM, admittance model and capacitance model.

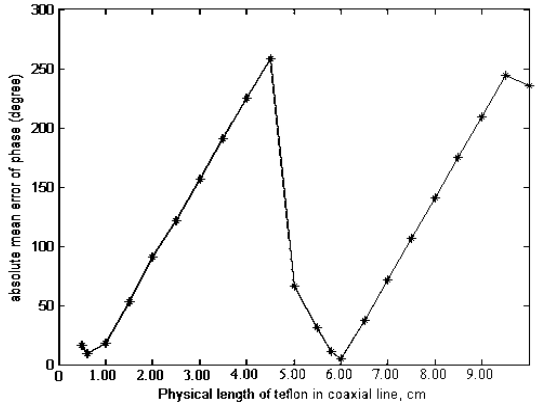

Fig. 14. Length of coaxial line with its phase error of reflection coefficient.

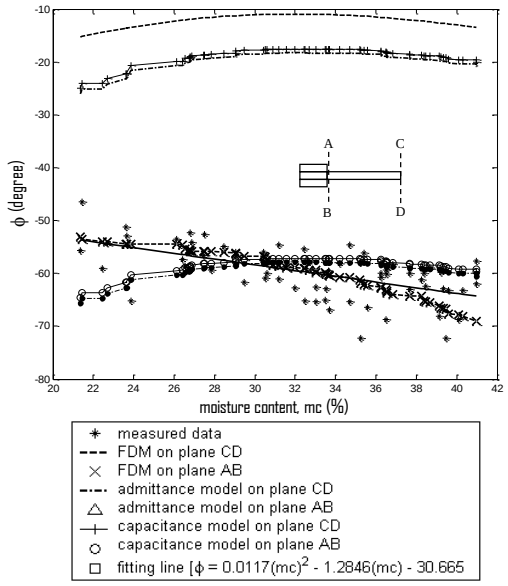

Fig. 15. Region 1 of Fig. 13.

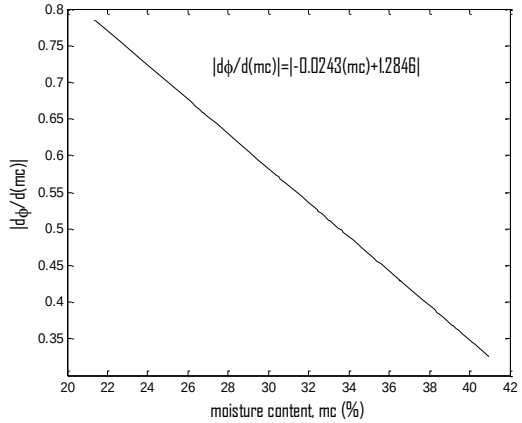

Fig. 16. Sensitivity, $|d\phi/d(mc)|$ for mc range between 20% to 40% (region 1).

Figure 17 represents region 2 in Fig. 13. The mc range 40% to 90% is within week 12 to week 16 after anthesis. During this period, the condition in Fig. 17 is similar to Fig. 11 because they show a similar trend. The water content starts to decrease, whereas oil content starts to rise in week 16 after anthesis. It can be observed that the error of FDM, admittance model and capacitance model are larger than the case in Fig. 15, namely 8.51 degrees, 22.29 degrees and 18.97 degrees. In Fig. 15, FDM still shows the best agreement with measured data. It has the smallest error compared with admittance model and capacitance model. Unlike the case in Fig. 15, the results of admittance model and capacitance model deviated from measured phase in mc range from 40% to 90%. The admittance model and capacitance model have larger mean phase error, namely 22.29 degrees and 18.97 degrees, respectively. The fitting equation that represents the trend of measured phase is $\phi = 0.0015(\text{mc})^2 - 0.9145(\text{mc}) - 27.928$ as shown in Fig. 17, while the relationship between sensitivity and mc is $|d\varphi / d(mc)| = (0.0030)(\text{mc}) - 0.9145$.

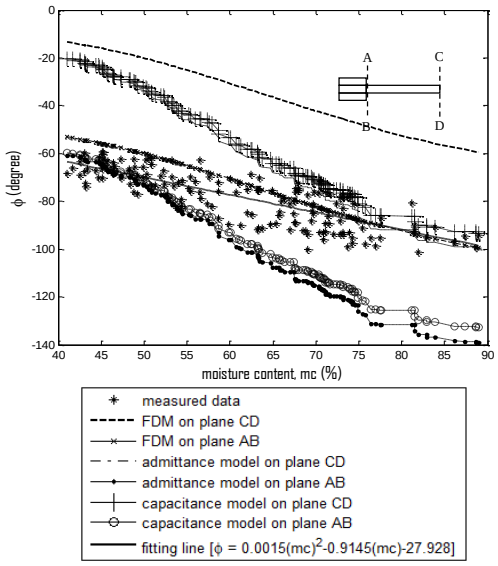

Fig. 17. Region 2 of Fig. 13.

For moisture content from 40% to 90%, the sensitivity decreases from 0.79 to 0.65. However, the range of sensitivity in Fig. 16 is from 0.3 to 0.8. The measured phase in the moisture content from 40% to 90% shows higher sensitivity than in Fig. 16. This can be explained by referring to Fig. 4. In Fig. 4, the ε' and ε" increase drastically when the moisture content is greater than 40%. The negative phase of reflection coefficient increases when the complex permittivity increases as well. The sensitivity of phase $\left(\left|\frac{d\phi}{d(mc)}\right|\right)$

shows higher than the magnitude in region 2 (Fig. 17). This implies that a small change in moisture content can be easily detected by the phase of reflection coefficient when compared with magnitude of reflection coefficient. This can help to estimate the moisture content accurately [23].

In region 2 where mc > 40%, the sensitivity is higher than region 1. The sensitivity can be expressed as $\left|\frac{d\phi}{d(mc)}\right| = \left|-0.0245(mc)+2.25\right|$ (Fig. 18). It is in line with the response of moisture content to the weeks after anthesis as shown in Fig. 2, where the variation of mc becomes drastic when mc > 40%.

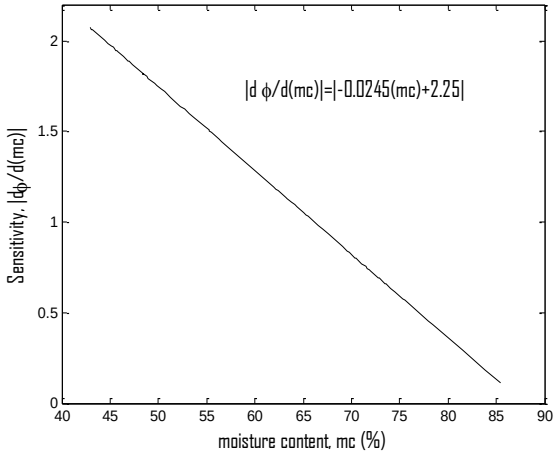

Fig. 18. Sensitivity, $\left|\frac{d\phi}{d(mc)}\right|$ for mc range that exceeds 40%.

IV. CONCLUSION

In this work, the complex reflection coefficient was analyzed computationally with FDM on an aperture coaxial sensor. The accuracy of this analysis was investigated by comparing calculated (FDM, the admittance model and the capacitance model) with measured reflection coefficients (measured using a Vector Network Analyzer). Figures 7 and 13 indicate that the FDM was more accurate than the admittance model and the capacitance model.

REFERENCES

[1] C. W. S. Hartley, *The Oil Palm*. 3rd ed., Longman, London, 1988.

[2] C. H. Teoh, "The Palm Oil Industry in Malaysia: From Seed to Frying Pan," *Report of WWF Malaysia*, pp. 5, 2002.

[3] A. Tola and T. B. Aishat, "Palm fruit in traditional African food culture," *Asia Pacific J. Clin. Nutr*., vol. 12, no. 3, pp. 350-354, 2003.

[4] S. Y. Choong, S. Abbas, A. R. Shariff, R. Halim, M. H. S. Ismail, R. Yunus, S. Ali, and F. R. Ahmadun, "Digital image processing of oil palm fruits," *International Journal of Food Engineering*, vol. 2, iss. 2, Article 7, 2006.

[5] Z. May and M. H. Amaran, "Automated oil palm fruit grading system using artificial intelligence," *International Journal of Video & Image Processing and Network Security IJVIPNS-IJENS*, vol. 11, no. 03, pp. 30-35, 2011.

[6] A. Ariffin, "Fundamental aspects of oil and fats, *In Improving Oil Extraction Rates in Palm Oil Mills, Sabah: CEPP and UTM*, 2005.

[7] A. Ariffin, "Biochemical aspects of ripeness standard," *In Proceedings of the Symposium on Impact of Pollination Weevil on the Malaysian Oil Palm Industry, Kuala Lumpur: Palm Oil Research Institute of Malaysia*, 1984.

[8] A. Ariffin, S. R. Mat, M. Banjari, and O. W. E. Wan, "Morphological changes of the cellular component of the developing palm fruit (Tenera: Elaeis Guineesis)," *Palm Oil Research Institute of Malaysia Bulletin*, vol. 21, pp. 30-34, 1990.

[9] K. Khalid and Z. Abbas, "A microstrip sensor for determination of harvesting time for oil palm fruits (Tenera: Elaeis Guineesis)," *J. Microwave Power and Electromag. Energy*, vol. 27, pp. 3-10, 1992.

[10] Z. Abbas, Y. K. Yeow, A. H.Shaari, J. Hassan, E. Saion, K. B. Khalid, and A. Zakaria, "Fast and simple technique for determination of moisture content in oil palm fruits," *Jpn. J. Appl. Phys*., vol. 44, no. 7A, pp. 5272-5274, 2005.

[11] K. Y. Lee, Z. Abbas, N. S. Mohamed Dan, and K. Y. You, "Portable microwave instrumentation system for determination of moisture content in oil palm fruits," *Jpn. J. Appl. Phys*., vol. 48, 2009.

[12] Z. Abbas, K. Y. You, A. H. Shaari, K. Khalid, J. Hassan, and E. Saion, "Complex permittivity and moisture measurements of oil palm fruits using an open-ended coaxial sensor," *IEEE Sensor Journal*, vol. 5, no. 6, pp. 1281-1287, 2009.

[13] S. Khandige and D. Misra, **"**Characterization of the layered dielectrics using an open-ended coaxial line sensor," *In Proceeding of* Conference *on Precision Electromagnetic Measurements Digest*, pp. 65-66., 27th June-1st July, 1994.

[14] R. C. Rumpf, "Simple implementation of arbitrarily shaped total-field/scattered-field regions in finite-difference frequency-domain," *Progress in Electromagnetics Research B*, vol. 36, pp. 221-248, 2012.

[15] V. Demir, "Graphics processor unit (GPU) acceleration of finite-difference frequency-domain (FDFD) method," *Progress in Electromagnetics Research M*, vol. 23, pp. 29-51, 2012.

[16] I. Karuppannan, O. Omar, and A. Ariffin, "Profiles of biochemical changes during the development of oil palm mesocarp (Elaesis Guineensis)," *Proc.*

Mal. Biochem. Soc. Conference, vol. 11, pp. 129-134, 1986.

[17] E. M. Cheng, M. F. B. A. Malek, M. Ahmed, K. Y. You, K. Y. Lee, and H. Nornikman, "The use of dielectric mixture equations to analyze the dielectric properties of a mixture of rubber tire dust and rice husks in a microwave absorber," *Progress in Electromagnetics Research, PIER*, vol. 129, pp. 559-578, 2012.

[18] A. Nyshadham, C. L. Sibbald, and S. S. Stuchly, "Permittivity measurements using open-ended sensors and reference liquid calibration – An uncertainty analysis," *IEEE Trans. Microwave Theory Tech*., vol. 43, pp. 1986-1989, 1992.

[19] K. Y. Lee, Z. Abbas, Y. K. Yeow, M. D. Nur Sharizan, and C. E. Meng, "In situ measurements of complex permittivity and moisture content in oil palm fruits," *Eur. Phys. J. Appl. Phys*., vol. 49, pp. 31201, 2010.

[20] M. A. Jusoh, Z. Abbas, J. Hassan, B. Z. Azmi, and A. F. Ahmad, "A simple procedure to determine complex permittivity of moist material using standard commercial coaxial sensor," *Meas. Sci. Review*, vol. 11, no. 1, pp. 19-22, 2011.

[21] V. M. Serdyuk, "Dielectric study of bound water in grain at radio and microwave frequencies," *Progress in Electromagnetics Research, PIER*, vol. 84, pp. 379-406, 2008.

[22] N. Marcuvtiz, *Waveguide Handbook*. Boston, MA: Boston Tech. Pub., pp. 213-216, 1964.

[23] K. Y. You, Z. Abbas, and K. Khalid, "Application of microwave moisture sensor for determination of oil palm fruit ripeness," *Meas. Sci. Review*, vol. 10, no. 1, pp. 7-14, 2010.

[24] A. Taflove, *Computational Electrodynamics: The Finite Difference Time Domain Method*. Boston, MA: Artech House, 1995.

[25] M. F. Zainuddin, Z. Abbas, M. H. M. Hafizi, M. A. Jusoh, and M. H. H. Razali, "Monopole antenna technique for determining moisture content in the Dioscorea hispida tuber," *Australian Journal of Crop Science, AJCS*, vol. 7, no. 1, pp. 1-6, 2013.

[26] A. H. Ali, Z. B. Abbas, J. B. Hassan, A. B. Jusoh, and R. B. M. Zahari, "Microwave antenna sensing technique for determination of moisture content in Hevea latex from Hevea Brasiliensis tree," *Australian Journal of Crop Science, AJCS*, vol. 5, no. 11, pp. 1326-1333, 2011.

[27] F. Ansarudin, Z. Abbas, J. Hassan, N. Z. Yahaya, and M. A. Ismail, "A simple insulated monopole sensor technique for determination of moisture content in *Hevea* rubber latex," *Meas. Sci. Review*, vol. 12, no. 6, pp. 249-254, 2012.

[28] K. Y. You, H. K. Mun, L. L. You, J. Salleh, and Z. Abbas, **"**A small and slim coaxial probe for single rice grain moisture sensing," *Sensors*, vol. 13, pp. 3652-3663, 2013.

Ee Meng Cheng was born in 1980. He obtained his B.Sc. (Honours) - Instrumentation Science in Universiti Putra Malaysia in 2004. He pursued his M.Sc. in Wave Propagation at the Institute for Mathematical Research in 2005 at Universiti Putra Malaysia and his Ph.D. in Microwave at the Faculty of Science in 2007 at Universiti Putra Malaysia. Recently, he is a Senior Lecturer in School of Mechatronic Engineering, Universiti Malaysia Perlis. His main personal research interest is in the computational electromagnetic modeling, microwave dielectric spectroscopy, wave propagation in RF & microwave and microwave sensors development for food and agricultural applications.

Zulkifly Abbas was born in Alor Setar, Malaysia, in 1962. He received the B.Sc. degree with honors in Physics from the University of Malaya, Kuala Lumpur, in 1986, the M.Sc. degree in Microwave Instrumentation from the Universiti Putra Malaysia (UPM), Serdang, in 1994, and the Ph.D. degree in Electronic and Electrical Engineering from the University of Leeds, Leeds, U.K., in 2000. He is currently an Associate Professor with the Department of Physics, UPM, where he has been a Faculty Member since 1987. His main personal research interest is in the theory, simulation, and instrumentation of electromagnetic wave propagation at microwave frequencies focusing on the development of microwave sensors for agricultural applications.

Mohd Fareq bin Abdul Malek obtained his B.Eng. (Honours) - Electronic and Communication Engineering in The University of Birmingham, United Kingdom in 1994. He pursued his M.Sc. (Eng.) in Microelectronic Systems and Telecommunications at The University of Liverpool, United Kingdom in 2003 and Ph.D. Electrical Engineering (Radio Frequency and Microwave) on 2005 in The University of Liverpool, United Kingdom. Recently, he is an Associate Professor in Faculty of Engineering and Information Sciences, University of Wollongong in Dubai. His main personal research interest is in electron maser, antenna design, embedded computing and microwave absorber development.

Kim Yee Lee was born in Muar, Johor, Malaysia. He received his B.Sc. Physics, M.Sc. (Microwaves), and Ph.D. (Microwaves) from Universiti Putra Malaysia in year 2002, 2004, and 2008 respectively. In December 2007, he joined Universiti Tunku Abdul Rahman as a Lecturer in Department of Electronics and Electrical Engineering. His areas of research include microwave measurement technique, microwave circuit and instrumentation, control and automation, material properties measurement, and instrumentation calibration.

Kok Yeow You was born in 1977. He obtained his B.Sc. Physics (Honours) degree in Universiti Kebangsaan Malaysia in 2001. He pursued his M.Sc. in Microwave at the Faculty of Science in 2003 and his Ph.D. in Wave Propagation at the Institute for Mathematical Research in 2006 at Universiti Putra Malaysia. Recently, he is a Senior Lecturer at Radio Communication Engineering Department, Universiti Teknologi Malaysia. His main personal research interest is in the theory, simulation, and instrumentation of electromagnetic wave propagation at microwave frequencies focusing on the development of microwave sensors for agricultural applications.

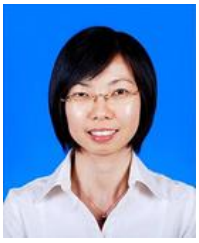

Shing Fhan Khor was born in 1982. She obtained her B.Sc. with Edu. (Honours) - Physics in Universiti Putra Malaysia in 2007. She pursued her Ph.D. in Materials Science at the Faculty of Science in 2011 at Universiti Putra Malaysia. Recently, she is a Senior Lecturer at School of Electrical Systems Engineering, Universiti Malaysia Perlis (UniMAP). Her main personal research interest is in the glass science and focusing on dielectric, optical, mechanical and thermal properties.

Jumiah Hassan is currently an Associate Professor with the Department of Physics, Faculty of Science, UPM. Her main research interests include dielectric physics, materials science, and condensed matter physics.

Hishammudin Zainuddin is currently an Associate Professor with the Department of Physics, Faculty of Science, UPM. His main research interests include Theoretical Physics, Quantum Physics, Geometry and Topology.